NRAO Electronics Division Technical Note No. 193

Cancellation of TV Interference
December 27, 2002

D. Anish Roshi

NRAO Electronic Division Technical Note, EDTN-193

Cancellation of TV Interference

D. Anish Roshi

National Radio Astronomy Observatory[1], Box 2, Green Bank, WV 24944, USA, aroshi@nrao.edu

Abstract

Radio frequency interference (RFI) is increasingly affecting radio astronomy research. A few years ago, active research to investigate the possibility of observing in the presence of interference using RFI mitigation techniques was initiated. Here, we discuss techniques to suppress interference due to television (TV) transmission. A good fraction of the radio frequency spectrum in the VHF (54 – 88 and 174 – 216 MHz) and the UHF (470 – 794 MHz) bands are allocated for TV transmission. These frequency ranges can be of potential importance for astronomical observations such as observations of redshifted spectral lines and the spectral signature of the epoch of reionization. This paper presents techniques to suppress interference due to synchronization signals in TV transmission. A combination of noise-free modeling of the synchronization signals and adaptive filtering is used for suppressing the interference. The measured *lower limit* on RFI rejection using this technique on TV synchronization signal is about 12 dB. We also present a simple, but interesting, technique to suppress double sideband (DSB) amplitude modulated interference. We show that using this technique a spectral feature of astronomical interest located either at the upper or lower sideband side of the DSB interference can be observed with reasonable signal-to-noise ratio even in the presence of the interference.

---

1 Introduction

Radio frequency interference (RFI) is increasingly affecting radio astronomy research. The need to find ways to deal with RFI is becoming more urgent because: (1) increase in research interests outside the allocated frequency bands for radio astronomy, (2) need to do higher sensitivity observations which are often limited by RFI and (3) growing technological resources which are becoming potential sources of increased radio frequency interference. Currently, less than 2 % of the 30 to 30000 MHz frequency range is reserved for passive use such as radio astronomy. Another 1.5% is given primary or secondary protection and is shared with other spectral activities. Most of the spectral windows that are protected based on the frequencies of spectral lines of astrophysical interest are allocated around the rest frequencies of the transitions. Redshifted spectral transitions therefore can fall outside the protected bands. Study of redshifted transitions are important to understand the origin and evolution of the universe. Such observations have to be made in spectral bands where RFI may be present.

The requirements of future astronomy research cannot be fulfilled by spectrum regulations alone. Therefore, active research was started a few years ago to investigate the possibility of doing radio astronomy observations in the presence of interference using RFI mitigation techniques (Fisher 2002, Fridman & Baan 2001 and references therein). Several techniques have been tried for suppressing RFI from the output of single dish radio telescope. Fisher (1997) made use of the polarized nature of the man made RFI to subtract interference from the telescope output. This technique gave on the average 8 dB of RFI suppression. Barnbaum & Bradley (1998) developed a real-time adaptive cancellation technique to suppress interference. They used a low gain reference antenna for picking up the RFI. The reference antenna output along with an adaptive filter is used to suppress the RFI in the telescope output. Laboratory tests of the adaptive canceler have achieved suppression of 72 dB, though field test with multiple interference gave a rejection of only 25 dB. Ellingson, Bunton & Bell (2001) developed a parametric signal modeling technique to suppress interference due to GLONASS (*Global'naya Navigatsionnaya Sputnikovaya Sistema*) signals. Tests of the method done on freely available data contaminated with RFI, made available by Bell et. al.(2000), were highly successful. They achieved a spectral dynamic range of 30 dB. While the above two mitigation techniques are implemented in the voltage domain, Briggs, Bell & Kesteven (2000) developed a post-correlation

technique, which essentially works on the power domain (i.e. after detection). This method makes use of cross power spectrum of RFI signals from a reference antenna pointing at the RFI source and the closure relation of amplitude and phase of the RFI signal in the reference antenna with the interference in the contaminated astronomical signal. The method has been successfully tested on the freely available data provided by Bell et. al.(2000). The deviation of the probability distribution of the output of a telescope from normal distribution in the presence of RFI was also used to excise interference (Fridman 2001).

RFI rejection achieved in techniques developed till now, however, are often not sufficient for sensitive radio astronomy observations. We feel that better rejection of RFI can be achieved by making use of the characteristics of the interfering signal. With this aim, we studied the characteristics of television (TV) signals and developed techniques to suppress interference due to these signals. The characteristics of TV signals are used to develop a noise-free model of the interfering signal. Such noise-free model can either be subtracted (after scaling it appropriately) from the data or can be used as a reference input to an adaptive filter. Rejection achieved in adaptive RFI suppression techniques are limited by the "interference-to-noise ratio" in the reference input (Barnbaum & Bradley 1998). Using a noise-free model as the reference input to an adaptive filter therefore can provide higher rejection.

The motivation to suppress TV signals is that a considerable fraction of the radio frequency spectrum in the VHF (54 – 88 and 174 – 216 MHz) and the UHF (470 – 794 MHz) bands are allocated for TV transmission. These frequency ranges can be of potential importance for astronomy for a variety of observations. Examples are: (1) Low frequency radio recombination lines of carbon from Galactic interstellar medium are expected to be observed in absorption at frequencies < 100 MHz (Roshi, Kantharia & Anantharamaiah 2002 and references therein) (2) the signature of reionization of the Universe is expected as a sharp step in the spectrum of the sky due to red-shifted HI 21-cm line emission anywhere in the frequency range ~ 70 to 240 MHz (Shaver et. al. 1999). Developing techniques to suppress TV signals are thus important for doing such observations in the presence of the interfering signals.

This paper presents techniques to suppress synchronization signals in TV interference. The suppression of the picture part of TV interference will be discussed elsewhere. In Section 2 we discuss briefly the characteristics of the TV signal and the data used for the present work. A technique to suppress

double sideband modulated interference is discussed in Section 3. Techniques to suppress interference due to synchronization signals components of the interfering signal is presented in Section 4.

2   Characteristics of TV signal and the data used for this work

The TV signal consists of picture and frame synchronization signals – referred to as composite video signal. The synchronization signals consist of horizontal and vertical synchronization (synch pulses) and blanking pulses and 8 to 10 cycles of the 3.58 MHz color sub-carrier ('color burst'; see Fig. 1). The picture part of the composite video signal consists of luminance (monochrome) and chrominance (color) components. The chrominance components are quadrature modulated on a sub-carrier of frequency 3.58 MHz. The total bandwidth of the composite signal is 4.5 MHz. The composite video signal is then vestigial sideband (VSB) modulated on a carrier for transmission. The VSB modulation retains about 28% of the lower sideband. The picture frame rate and other details of the composite video signal depend on the standard used for TV transmission. Here we use data with NTSC (National Television System Committee) standard.

The data for the present work were obtained from the output of a video player. The RF output of the video player was digitized and acquired using a commercial data acquisition system. The carrier frequency of the video player output was near 61.2 MHz and the data were bandpass sampled at 50 MHz rate with an 8 bit analog-to-digital converter. A contiguous set of 50 Mbytes of samples was stored in the computer hard disk. Interestingly, the video player output was double sideband (DSB) amplitude modulated. A VSB modulated signal was obtained by appropriately bandpass filtering the recorded data.

3   'DSB suppressor'

Since the TV signal in the recorded data is DSB modulated, a technique to suppress DSB modulated signal is first tried. Consider a spectral feature of astronomical interest (for example, a red-shifted HI feature) at the upper sideband side of a DSB modulated interference (see Fig. 2). The output of

the radio telescope can be written as

$$y(t) = I_c \cos(\omega_c t) \left[1 + I_m \cos(\omega_m t)\right] + n(t), \qquad (1)$$

where I_c and ω_c are respectively the amplitude and angular frequency of the carrier signal, I_m and ω_m are respectively the amplitude and angular frequency of the modulating signal and $n(t)$ is the astronomical signal. For simplicity, we consider only one Fourier component of the modulating signal. Multiplying $y(t)$ with $\sin(\omega_c t)$ gives

$$y'(t) = \frac{I_c}{2}\sin(2\omega_c t) \left[1 + I_m \cos(\omega_m t)\right] + n(t)\sin(\omega_c t). \qquad (2)$$

Equation (2) shows that interfering signal will be present only at $2\omega_c$ and not at the baseband after multiplication. The astronomical signal $n(t)$ is essentially a Gaussian random noise and can be written in the narrow band approximation as

$$n(t) = n_1(t)\sin(\omega_0 t) + n_2(t)\cos(\omega_0 t). \qquad (3)$$

Here $n_1(t)$ and $n_2(t)$ are Gaussian random variables and ω_0 is the center frequency of the frequency band used for observation. Multiplying $n(t)$ with $\sin(\omega_c t)$ therefore produces noise signals at $(\omega + \omega_c)$ and $(\omega - \omega_c)$ frequencies. The noise at $(\omega + \omega_c)$ will be contaminated by the interference. The noise at $(\omega - \omega_c)$ frequency is at the baseband which is now free of the RFI. However, at the baseband, the noise below ω_c folds back resulting in a degradation of the signal-to-noise ratio by 2 compared to the detection of the astronomical signal in single sideband mode in the absence of the interfering signal.

In reality, the phase of the carrier frequency changes with time due to a variety of reasons; for example propagation effects. This change has to be taken into account by the suppressor for effective RFI rejection. This is done by filtering the carrier signal from the output of the telescope and phase locking with an oscillator (see Fig. 3). The oscillator is then phase shifted by 90° and mixed with the telescope output. The mixer output is low-pass filtered to get the desired astronomical signal. We implemented a variation of this technique in MATLAB, where a Hilbert transform of the telescope output is taken first to convert it into an analytic signal (see Fig. 3). This signal is then multiplied with a complex oscillator, which is phase locked to the carrier. The output of the multiplier is now a complex signal. The real part of the complex output ('Real' output) is equivalent to that described above.

5

The imaginary part of the complex output ('Imaginary' output) is equivalent to the telescope output being multiplied by the oscillator signal with 0° phase shift with respect to the carrier – essentially a coherent detector.

3.1 Interference-to-noise ratio and RFI rejection

The RFI rejection achieved in the 'DSP suppressor' depends on how well the carrier phase can be tracked, which in turn will depends on the carrier-to-noise power ratio (INR_C) at the carrier filter (Fig. 3) output. To get an approximate relationship between the residual RFI power at the 'Real' output of the 'DSB suppressor' and the INR_C, we consider that the local oscillator output has a random phase modulation $\phi(t)$. The baseband output of the mixer with the assumption that $\phi(t) < 1$ rad is then given by

$$y''(t) = y(t)\sin(\omega_c t + \phi(t))$$
$$\simeq y'(t) + \phi(t)n(t)\cos(\omega_c t)$$
$$+\frac{\phi(t)}{2}\left[1 + I_m\cos(\omega_m t)\right], \tag{4}$$

where $y'(t)$ is defined by equation (2). The last term in equation (4) is the residual of the RFI at the baseband output. The power of the residual RFI P_{RFI} is (considering only frequency components > 0 Hz),

$$P_{RFI} = \langle\frac{I_m^2\cos^2(\omega_m t)\phi^2(t)}{4}\rangle \simeq \frac{P_m}{4}\langle\phi^2(t)\rangle, \tag{5}$$

where P_m is the power of the modulating signal. $\langle\phi^2(t)\rangle$ can be related to the phase error of the carrier filter output, $\phi_c(t)$, using the transfer function of a phase lock loop (PLL; Manassewitsch 1976),

$$\phi(t) = \phi_c(t) * h_{PLL}(t) \tag{6}$$

where $h_{PLL}(t)$ is an effective low-pass filter response of the PLL and the convolution operation is denoted by $*$. Using equation (6) and applying Rayleigh's theorem $\langle\phi^2(t)\rangle$ can be approximated as

$$\langle\phi^2(t)\rangle \simeq \frac{\langle\phi_c^2(t)\rangle}{B_{BP}}KB_{PLL} \tag{7}$$

where B_{BP} is the noise equivalent bandwidth of the carrier filter. To get equation (7) we considered the equivalent low-pass filter of the PLL is rectangular with gain $K^{1/2}$ and having a bandwidth B_{PLL}. Also, we considered

that the spectral power density of $\phi_c \simeq \frac{\langle \phi_c^2(t) \rangle}{B_{BP}}$, which is a good approximation if the receiver noise dominates over the phase noise of the carrier within the filter bandwidth B_{BP}. The noise power in the sidebands of the spectrum of a phase modulated signal is proportional to $\langle \phi_c^2(t) \rangle$, if we assume that $\phi_c \ll 1$. With this approximation,

$$INR_C = \frac{1}{\langle \phi_c^2(t) \rangle} \qquad (8)$$

Using equations (8) and (7), the residual RFI power in equation (5) can be written in terms of INR_C as

$$P_{RFI} \simeq \frac{P_m \, K \, B_{PLL}}{4 \, B_{BP} \, INR_C}. \qquad (9)$$

The above equation shows that the residual RFI power is inversely proportional to INR_C.

3.2 Performance and limitations of the 'DSB suppressor'

The performance of the 'DSB suppressor' is measured using the recorded data. Average spectra of the 'Real' and 'Imaginary' outputs are obtained (see Fig. 4) and compared to measure the rejection achieved. The measured *lower limit* on the interference rejection is $\sim$ 12 dB. The limitations of the 'DSB suppressor' are: (1) good suppression can be achieved only if both sidebands are of equal amplitude and their relative phase is as expected theoretically and (2) any non-DSB noise from the interfering source will degrade the system temperature of the radio telescope. From an observational point of view, the DSB suppressor is good for continuum observations. For spectroscopic observations, the spectral feature should be positioned either on the upper or lower side of the carrier frequency. Otherwise the spectral feature gets folded in frequency.

4 TV Synchronization Signal Suppressor

As mentioned earlier, the NTSC TV transmission retains only about 1.25 MHz of the lower sideband. Since the spectral power of the synch and blanking pulses increase by more than 10 dB in the frequency range 0 to 1 MHz

7

(see Fig. 5), the lower sideband in TV transmissions can be used to suppress this power using a 'DSB suppressor'. Thus, after passing the VSB modulated TV signal through the 'DSB suppressor' the 'Real' output consists of frequency components all above $\sim$ 1.25 MHz (see Fig. 6). These components include the color burst and the higher frequency (> 1.25 MHz) components of the synch and blanking pulses in addition to the picture signal.

4.1   Color Burst Suppressor

We first try to suppress the color burst in the 'Real' output by using a noise-free model of this signal. The color burst signal in the 'Imaginary' output, which is now considered as a reference signal, is used to make the noise-free model. The color burst is filtered out from the 'Imaginary' output and used to synchronize the phase of an oscillator (see Fig. 7). This is done every horizontal synch period where a color burst is present. The oscillator output is then multiplied by a 'window' function to generate the model (see Fig. 8). The position of the window function in time relative to the horizontal synch signal is estimated in sample numbers and used for synchronizing. The shape of the window function is initially estimated from the reference signal itself and held constant. We tried subtracting a scaled version of the noise-free model. However, this did not give good RFI rejection. The relatively poor RFI rejection is primarily due to changing shape of the weighting function at $\sim$ 30 % level. We then used the noise-free model as the reference signal for a three tap adaptive filter and the 'Real' output is used as the second (main) signal for the filter. New filter weights are computed only during the time interval when the color burst amplitude is not changing rapidly. Controlling the weights in this fashion has given the best performance for the canceler. Fig. 9 shows a typical output of the color burst suppressor.

Note that the noise-free model of the color burst is generated by phase synchronizing an oscillator to the data. As shown in Section 3.1, in such phase synchronization techniques, the phase noise of the model should depend on the interference-to-noise ratio of the reference signal. Since the timing and frequency of the color burst are well specified, the generation of the noise-free model can be made using a state model. This will be attempted in future (see Section 5 for further discussion on state model).

8

4.2 Synch and Blanking Pulse Suppressor

After passing the 'Real' output through the 'color burst suppressor', what remains are the residuals of synch and blanking pulses. To get a noise-free model for the residual, the synch and blanking pulses from the 'Imaginary' output are filtered out first for each horizontal synch period (see Fig. 10). Passing the derivatives of these pulses through a threshold detector gives the time of occurrence of these pulses. A 'delta' function model of the residuals is generated using this information. This model is then convolved with a shaping function, which is determined initially from the 'Imaginary' output (see Fig. 11). The noise-free model is then scaled and subtracted from the 'Real' output. The scaling factor is adjusted manually to get the best suppression. A typical output after passing the signal through the color burst and synch and blanking pulse suppressors is shown in Fig. 12.

4.3 Performance of the TV Synchronization Signal Suppressor

The performance of the synchronization signal suppressors is tested using a data set with no picture information. An average spectrum of the interference is obtained from the samples where the synchronization signals are present in the 'Real' output. To measure the RFI rejection achieved, a second average spectrum after suppressing the interference is obtained from the same set of samples. These spectra are shown in Fig. 13. The averaging is done over 8.6×10^6 samples, which corresponds to about 160 msec. No residual of the color burst is present in the second average spectrum, which gives a lower limit on the interference rejection of 12 dB. The average spectrum of the output of the suppressors is compared with a reference spectrum, which is obtained from the samples with no picture and synchronization signals. The comparison shows good agreement between the reference and average spectrum. The total power in the average spectrum of the output of the suppressors is, however, about 0.6 dB more than that of the reference spectrum. The excess power is mostly due to the inadequate suppression of the synch and blanking pulse residuals.

9

5   Discussion and Conclusion

In this paper, we present techniques to suppress synchronization signals in TV interference. A combination of noise-free modeling of interfering signal and adaptive signal processing is used for canceling the interference. The measured *lower limit* on interference rejection obtained using this technique is ~ 12 dB. The suppression technique made use of a reference signal to generate the noise-free model. Since the timing, frequency and shape of synchronization signals are well specified, a state model could be used to generate the noise-free model. However, information from reference signal needs to be incorporated in the state model generation for better RFI rejection. This could be implemented as a Kalman type filter. The state model could give a first approximation to the timing of the synchronization signals, but the signal shape (eg. shape function) and a better timing (eg. for delta function generation) need to be derived from the reference signal. The scaling factor in the synch and blanking pulse suppressor, which is currently held constant, should be changed adaptively using the reference data. Note that for short pulses, like the residual of the synch and blanking pulses in the 'Real' output, conventional adaptive algorithms cannot be used. We think a stochastic model for the picture component of the TV interference can be generated using the reference signal. This model could be then subtracted from the RFI contaminated data. This will be attempted in the future. The effectiveness of RFI suppression for different interference-to-noise-ratios of the reference signal also needs to be tested.

The TV synchronization signal suppressor also has the same limitations as the 'DSB suppressor' (see Section 3.2) as far as spectral line observations are concerned. The noise-free model of the TV interference can be modulated on a carrier and subtracted from the data to overcome this limitation. Thus no mixing of the signal with a carrier is needed. The carrier phase and amplitude in the telescope output should be matched before subtraction.

Our experience with TV interference cancellation indicates that a single cancellation technique may not give adequate suppression of interference for radio astronomy purposes. This is suggested by the fact that a combination of adaptive cancellation and noise-free modeling were needed to get better suppression of TV synchronization signals. Also, cancellation techniques have to be 'tuned' based on the characteristics of the interfering signal to get better suppression. This is again evident, for example, in the case of TV synch signal suppression, where we restricted updating the weights of the

adaptive filter.

Acknowledgment

References

Barnbaum, C., Bradley, F. R., 1998, AJ, 115, 2598

Bell, J. F., Ekers, R. D., Bunton, J. D., 2000, Proc. Astron. Soc. Aust., 17, 255

Briggs, F. H., Bell, J. F., Kesteven, M. J., 2000, AJ, 120, 3351

Ellingson, S. W., Bunton, J. D., Bell, J. F., 2001, ApJS, 135, 87

Fisher, R. J., 2002, NAIC-NRAO School on Single-Dish Radio Astronomy: Techniques and Applications, ASP conf. series, eds. S. Stanimirovic, D. R. Altschuler, P. F. Goldsmith, C. Salter

Fisher, R. J., 1997, Publ. Astron. Soc. Aust., 14, 96

Fridman, P. A., Baan, W. A., 2001, A&A, 378, 327

Fridman, P. A., 2001, A&A, 368, 369

Manassewitsch, V., 1976, Frequency Synthesizers Theory and Design, John Wiley & Sons, New York

Roshi, D. A., Kantharia, N. G., Anantharamaiah, K. R., 2002, A&A, 391, 1097

Shaver, P. A., Windhorst, R. A., Madau, P., de Bruyn, A. G., 1999, A&A, 345, 380
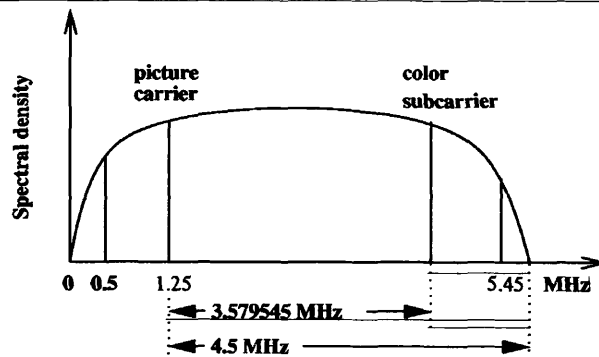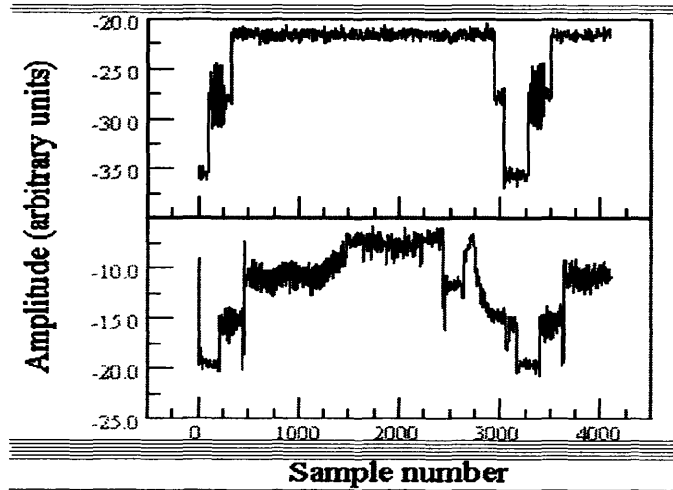
Figure 1: The top panel shows the synchronization signal with no picture information. The largest amplitude pulses are the horizontal synchronization pulses and the intermediate amplitude, wider pulses are the horizontal blanking pulses. The 3.58 MHz color burst is seen just after the synch pulses. The middle panel shows an example of the composite video signal; both picture and synchronization signals are present. A schematic of the spectral details of NTSC TV transmission is shown in the bottom panel. The composite video signal is VSB amplitude modulated on a carrier for transmission.

12
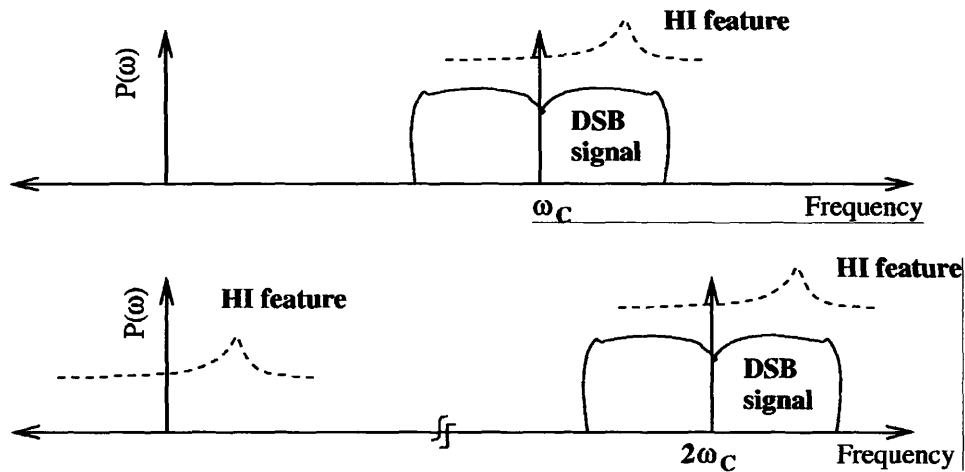
Figure 2: Schematic of the power spectrum of a double sideband (DSB) modulated interference along with an HI feature (top). The carrier frequency of the DSB interference is ω_c. The bottom figure shows a schematic of the spectrum after multiplying the RFI contaminated signal with the quadrature of the carrier of the DSB interference. The DSB interference is translated to $2\omega_c$ due to the multiplication. The astronomical signal will be present at the baseband as well as near $2\omega_c$ after multiplication. Thus low-pass filtering the multiplied output will give the astronomical signal without any RFI contamination. The spectral components of the astronomical signal and any noise below the carrier frequency, however, folds back in frequency at the baseband. This results in the degradation of signal-to-noise ratio by a factor of 2 compared to the case when the astronomical signal is observed in the absence of the DSB interference.

13
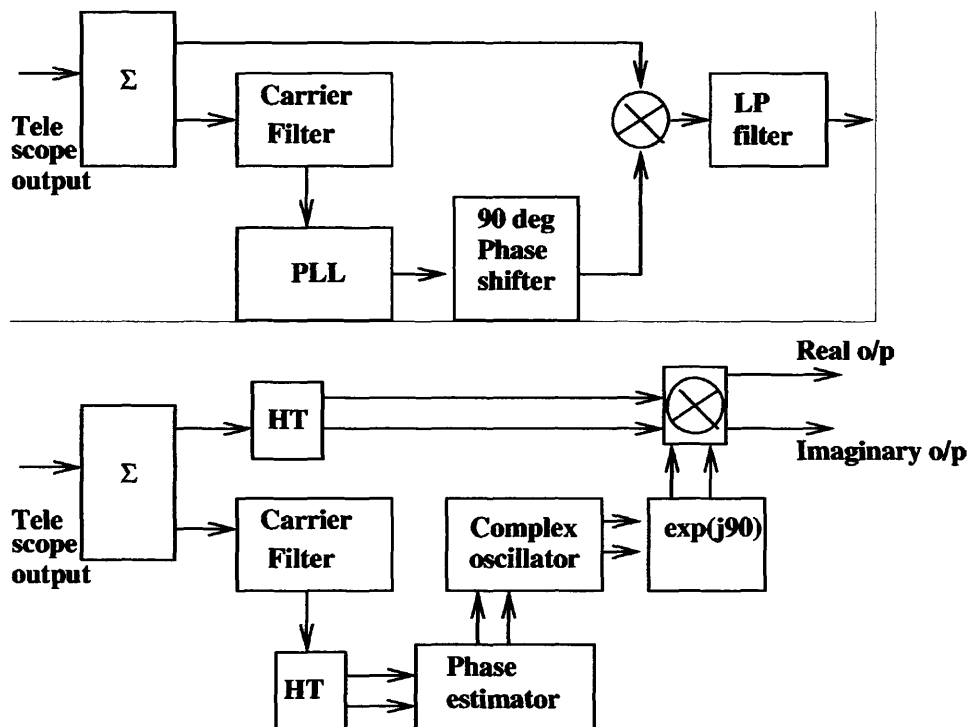
Figure 3: Block diagram of the 'DSB suppressor' is shown on the top. The block PLL implements a phase lock loop. A simplified block diagram of the implementation of 'DSB suppressor' in MATLAB is also shown in the bottom. The block HT takes the Hilbert transform of its input.
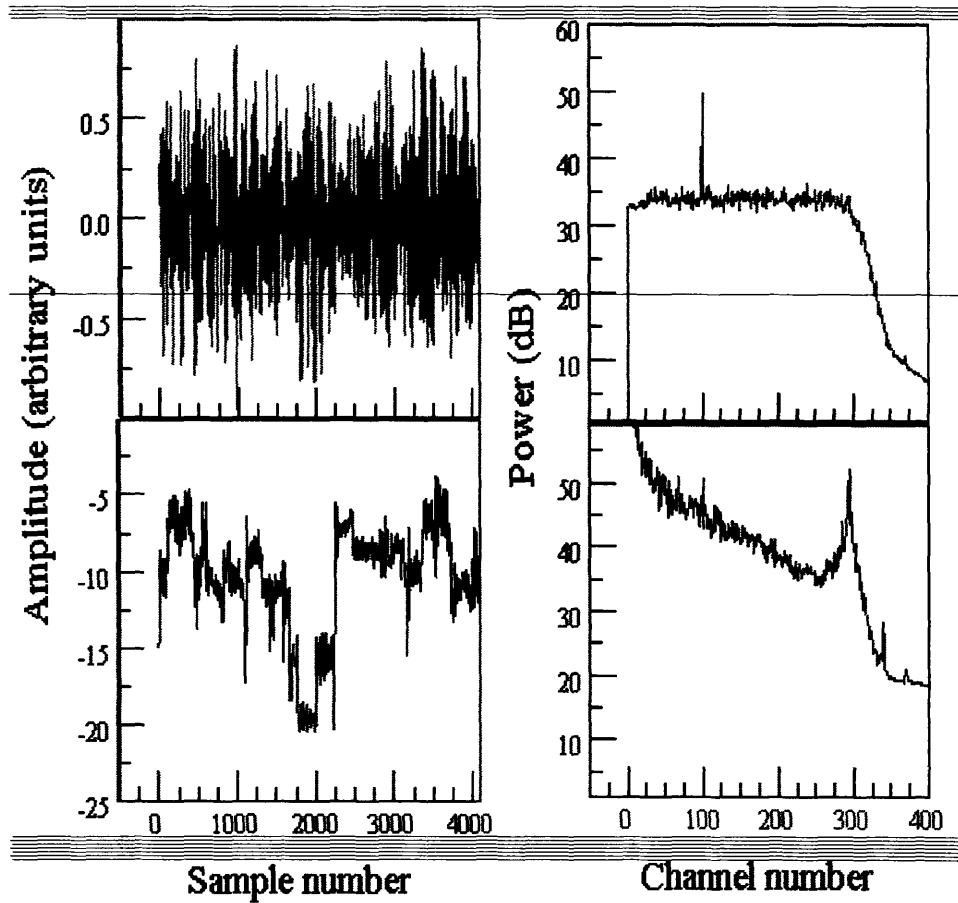
Figure 4: Time series of the 'Real' and 'Imaginary' output when the recorded signal is passed through the 'DSB suppressor' are shown on the top and bottom left panels respectively. The y-axis is the amplitude of the signal in arbitrary units and x-axis is the sample number. The average spectrum of the two outputs are shown on the right panels. The average is made over about 2×10^4 samples. The y-axis is the spectral power in dB and x-axis is channel number. The spectral resolution is about 12 KHz
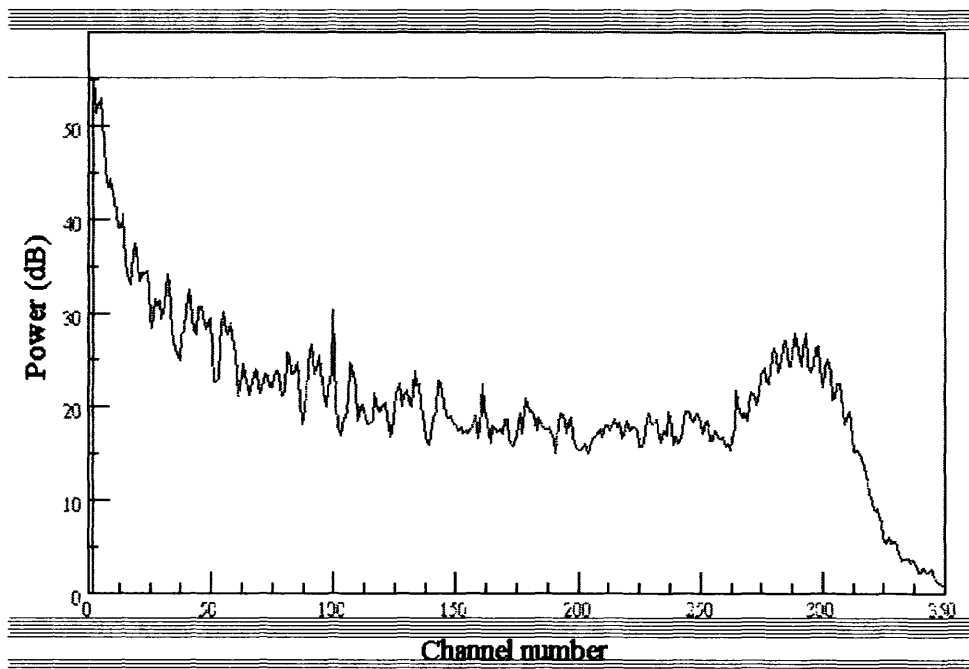
Figure 5: The spectrum of the synchronization signal. The excess power near channel 300 (3.58 MHz) is due to the color burst. The spectral power increases by more than 10 dB between 0 and 1.0 MHz. The resolution of the spectrum is about 12 KHz

16
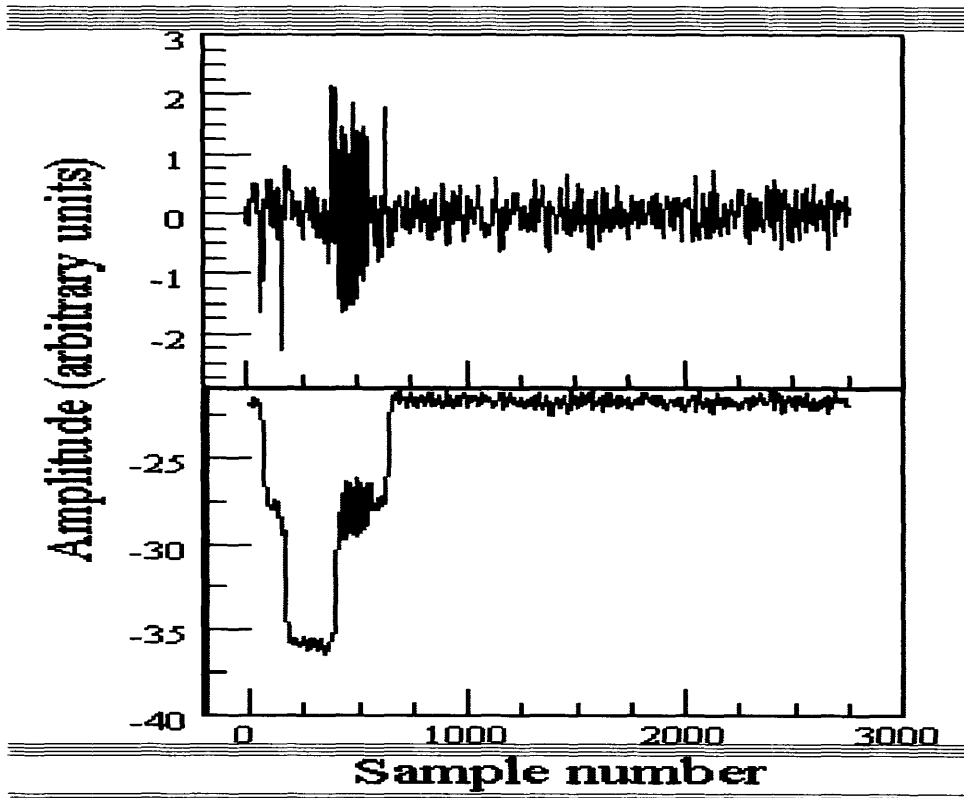
Figure 6: The top panel shows the time series of the 'Real' output of 'DSB suppressor' when a VSB modulated signal is passed through the suppressor. The bottom panel shows the time series of the 'Imaginary' output for the same input signal. Note that no picture information is present in the input signal.

17
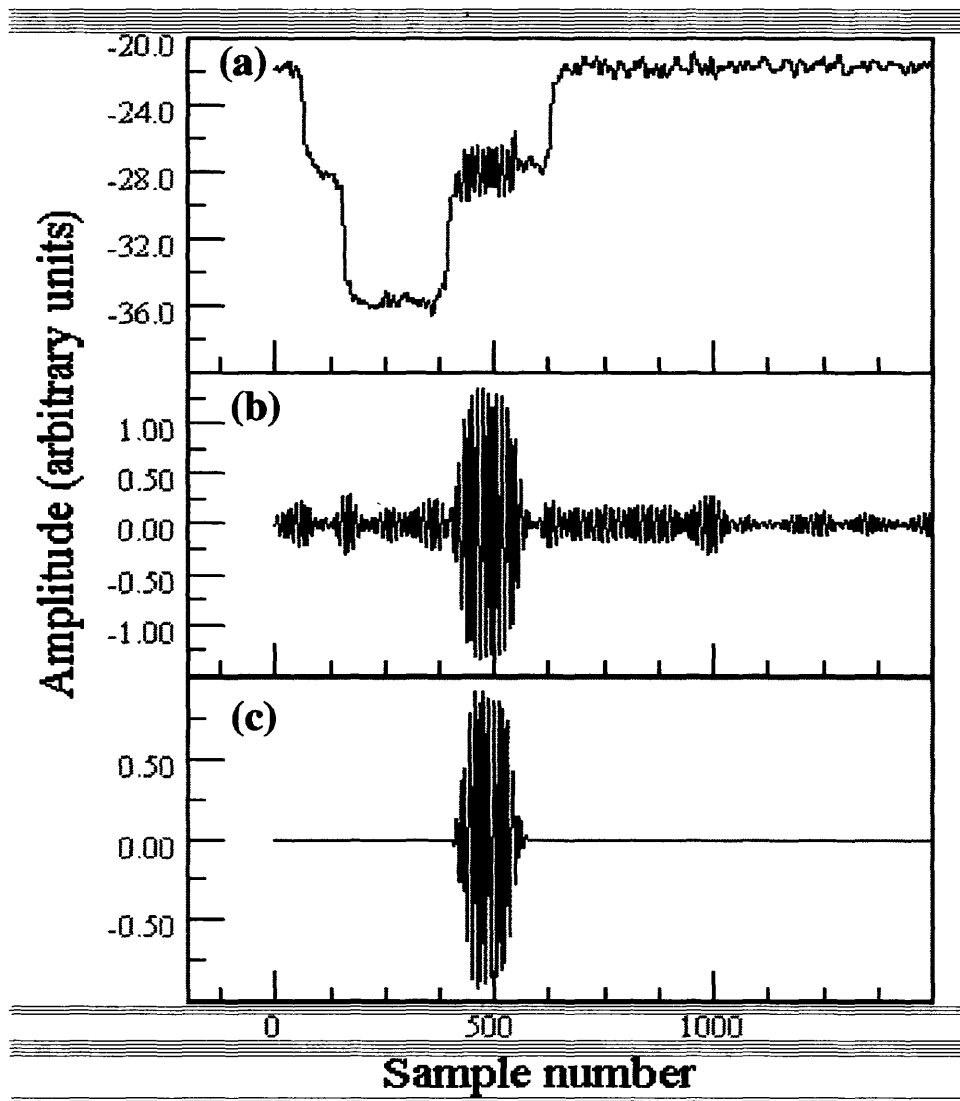
Figure 7: The top panel shows the 'Imaginary' output and the middle panel shows the high pass filtered output of the signal shown in the top panel. The synthesized noise-free model of the color burst is shown in the bottom panel.
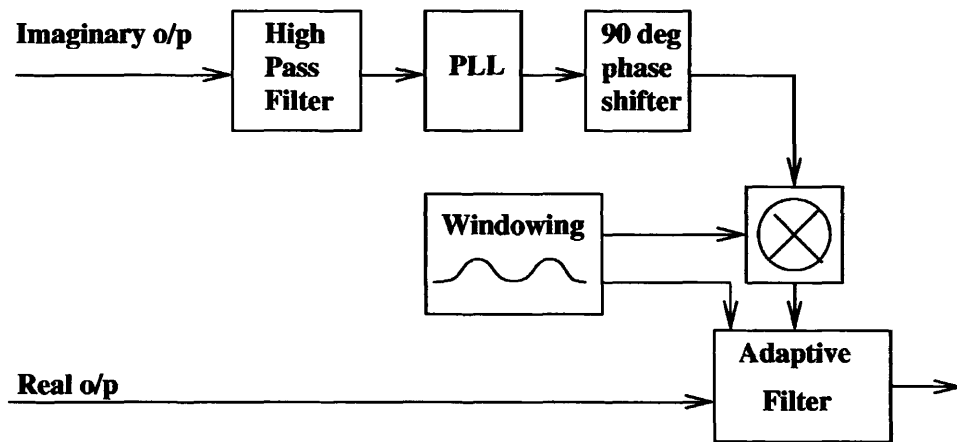
Figure 8: Block diagram of the color burst suppressor. The 90°phase shift is
needed at the output of the phase lock loop (PLL block) since the model is
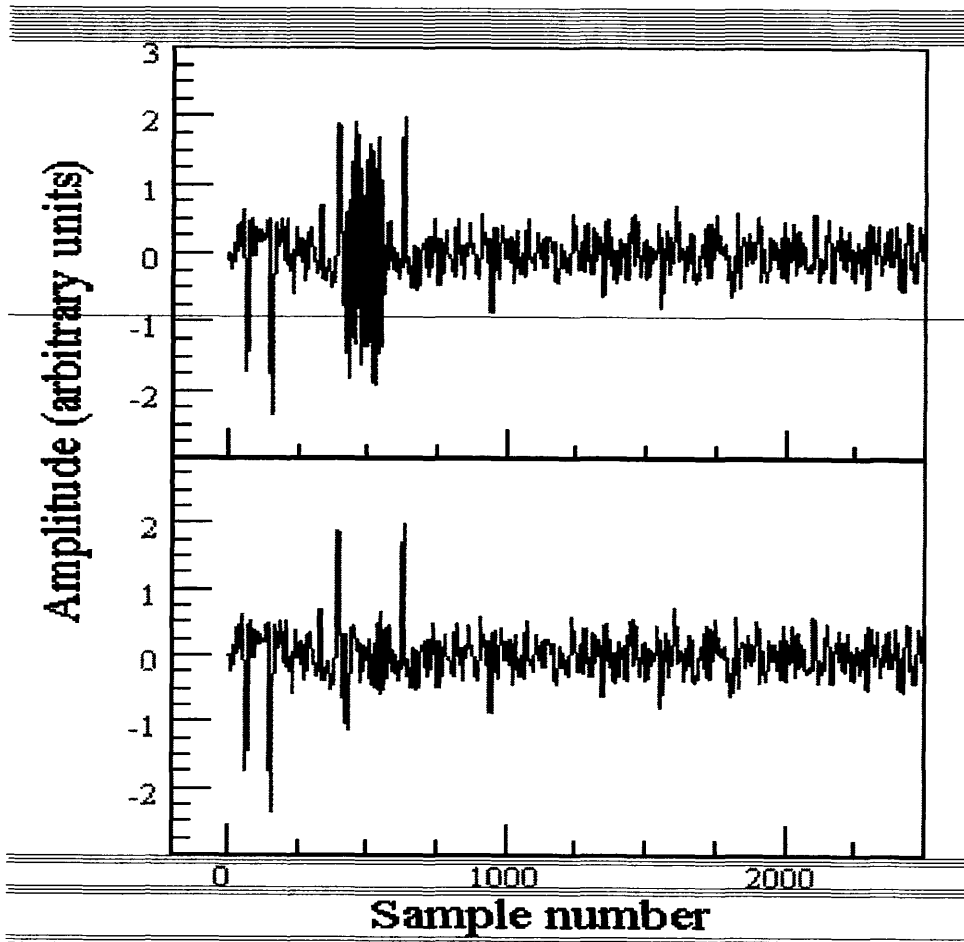subtracted from the 'Real' output.

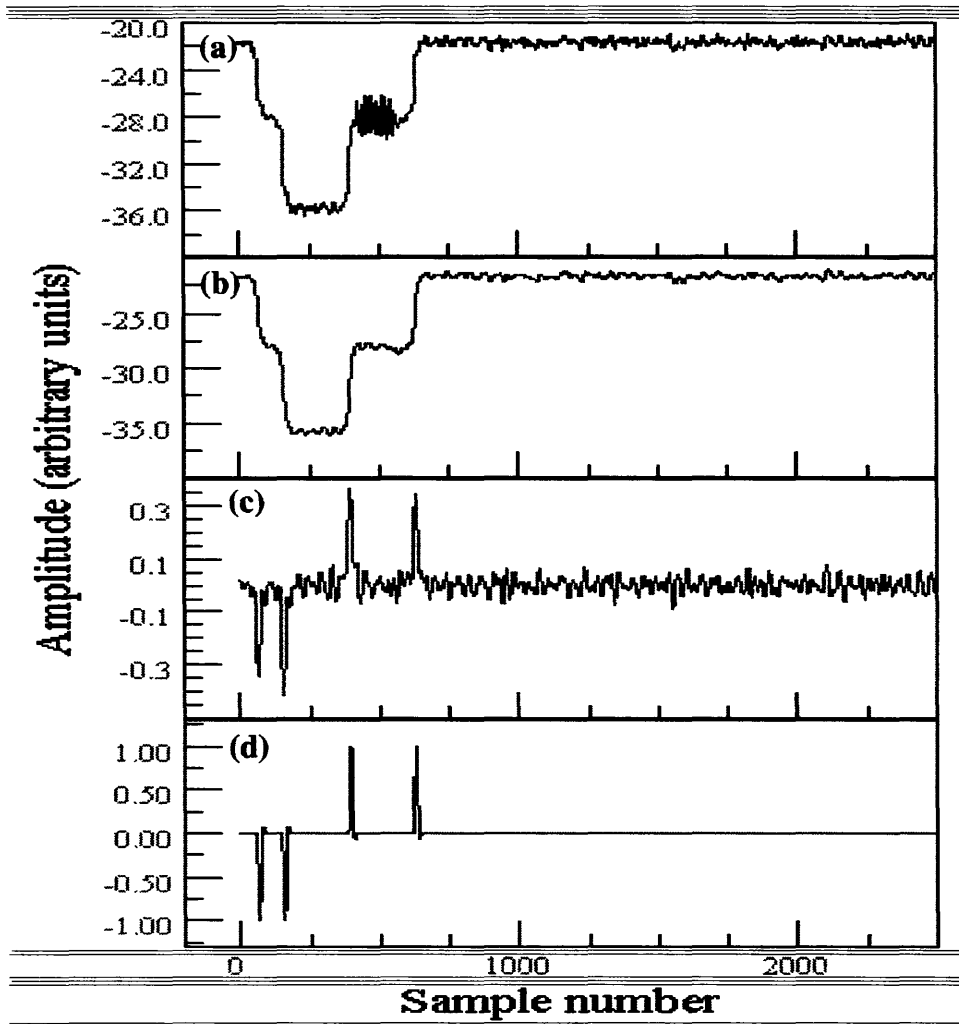Figure 9: Top and bottom panels show the input and output respectively of the color burst suppressor.

Figure 10: (a)Time series of the 'Imaginary' output. (b) Time series after passing the signal shown in (a) through a low-pass filter. The filter cutoff frequency is adjusted to reject the 3.58 MHz color burst. (c) The derivative of the signal shown in (b). (d) The noise free model of the synch and blanking pulse in the 'Real' output (see Section 3).
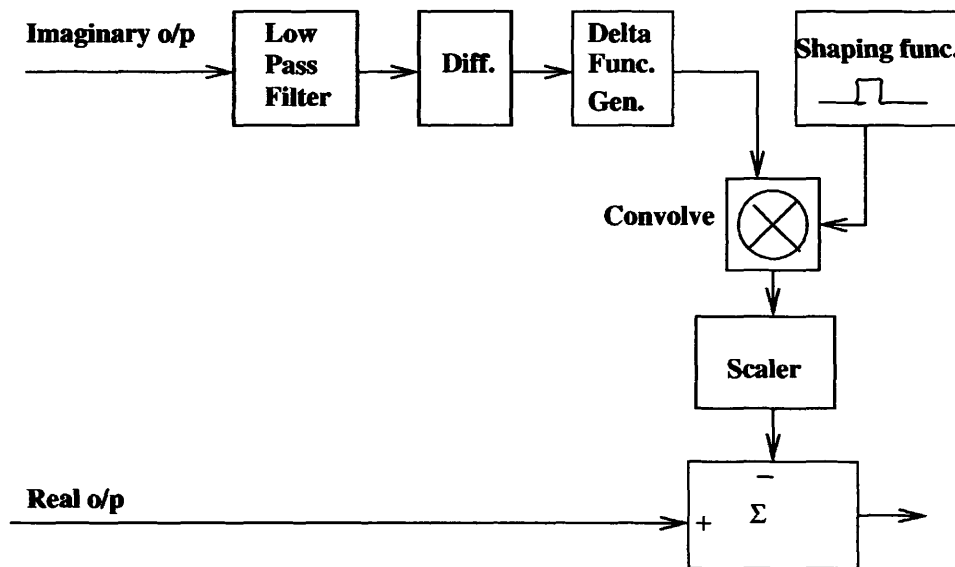
21

Figure 11: Block diagram of the synch and blanking pulse suppressor. At the output of the convolving block a noise-free model of the residual of synch and blanking pulses in the 'Real' output is obtained.
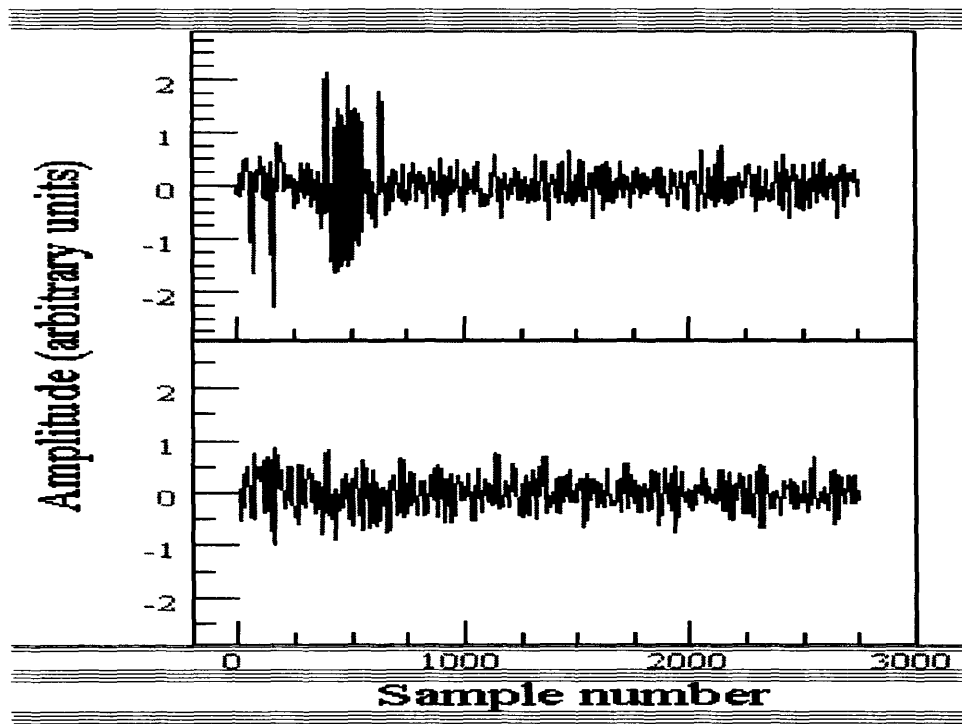
Figure 12: Top panel shows the time series of the 'Real' output. Bottom panel shows the signal after passing the 'Real' output through color burst and synch and blanking pulse suppressors.
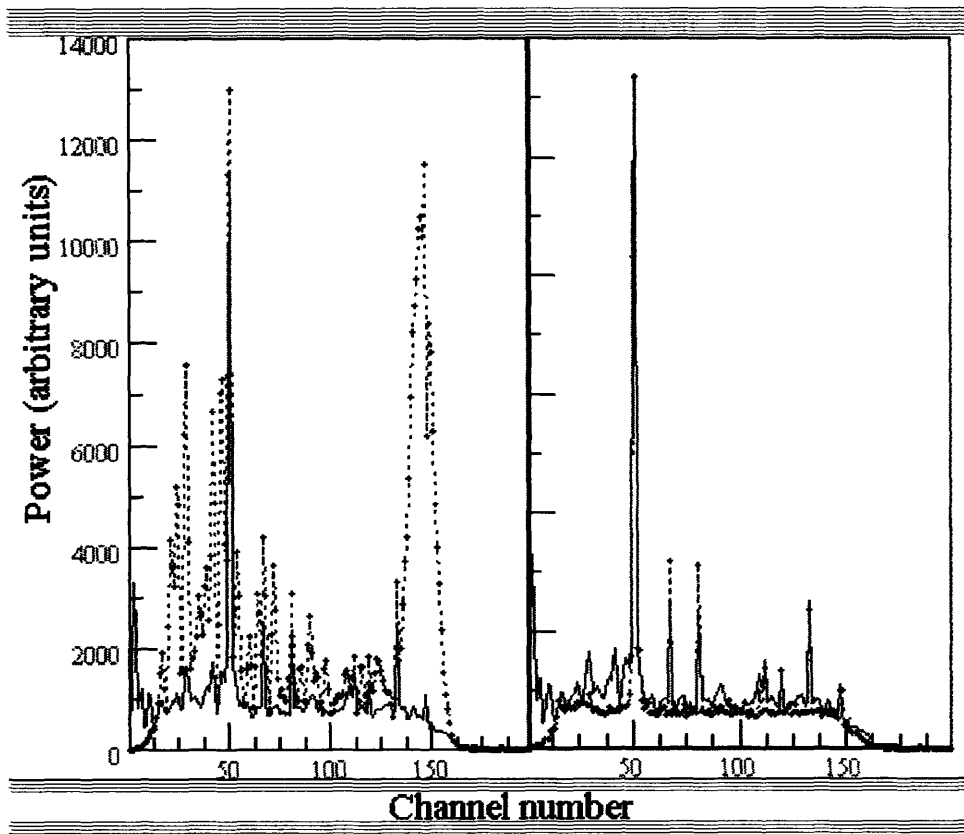
Figure 13: The average spectrum of the samples where interference is present at the 'Real' output is shown on the left panel in dotted line. The average spectrum obtained from the same set of samples after passing the data through the color burst and synch and blanking pulse suppressors is also shown on the left panel in solid line. The spectrum shown in dotted line on the right panel is a reference spectrum, which is obtained from the samples of the 'Real' output that do not have picture or synchronization signals. The average spectrum shown in solid line on the right panel is same as that shown on the left panel in solid line. The spectra are integrated over 6 x 10^6 samples ($\sim$ 120 msec). The spectral resolution is about 24 KHz.

24